A methodology to manage the complexity of a nonlinear multibody digital twin in railway applications

B. Auzanneau [1,2], **E. Sadoulet-Reboul** [1], **E. Foltête** [1], **G. Ham-Livet** [2], **S. Cogan** [1]
[1] Université de Franche-Comté, FEMTO-ST, Département de Mécanique Appliquée, France

[2] ALSTOM Transport SA, Le Creusot, France

Abstract
In the railway industry, digital twins based on nonlinear multibody simulations are developed to provide decision-making support for bogie design. A recurring question is to find an acceptable compromise between model complexity and computational burden to ensure an accurate representation of the global train dynamic behavior. The objective of the research work is to investigate different modeling strategies integrating the complexity of a physical model, and to discriminate between the effectiveness of these strategies in faithfully reproducing the dynamic responses of a structure. Two approaches are investigated to study a real yaw damper component of a motor bogie. Firstly, a rheological model representing the dynamic behavior of the damper is proposed and is integrated into dynamic simulations for sensitivity studies in order to identify the influential elements. In a second phase, an alternative model based on a multi-layer perceptron neural network is proposed to improve the computational efficiency of the digital twin.

1 Introduction and presentation of the study-case

The railway industry is a sector in which the search for performance and safety is an essential part of the design process. The growing use of digital twins is opening up new and unexplored avenues both in the preliminary design phase and in the final phase when railway vehicles are homologated. The bogies at the interface between the bodies and the track are critical components ensuring the stability and comfort of trains, and nonlinear multibody simulations provide assistance in the choice of suspension components at the design stage in order to guarantee good overall dynamic behavior of the train. A recurring challenge in the use of numerical simulations is to find an acceptable compromise between the complexity of the models and the associated computational burden. Simplified models may not accurately capture complex dynamic behavior, while models that are too detailed may incur prohibitive computational costs and be unusable in practice. In this context, the purpose of the research work is to investigate the level of model complexity required to validate the dynamic model of a railway bogie. This question is related to the problem of quantifying model-form error that has been a topic of recent investigations, for example [1]. A specific component of a bogie is considered, in this case a yaw damper, and the impact of the modeling of this component on the dynamic response of the bogie is investigated. The yaw damper is presented in Figure 1 (a). It is characterised using a traction-compression machine following the test management process defined at the ALSTOM Test Center : the right end of the damper is clamped and the left connected to an actuator such that the frequency, the amplitude and the speed of the excitation can be changed. A series of 30 tests are performed imposing a mono-harmonic displacement excitation at various amplitudes from $2\,\mathrm{mm}$ to $25\,\mathrm{mm}$, speeds from $0.085\,\mathrm{mm/s}$ to $255\,\mathrm{mm/s}$ and frequencies from $0.0068\,\mathrm{Hz}$ to $8.117\,\mathrm{Hz}$. Figure 1 (b) presents the normalized force-displacement hysteresis curves with the damper stroke along the horizontal direction and the resulting force along the vertical direction. All results in the article are presented in normalized values. The shapes of the curves are very far from a regular and symmetric ellipse which characterizes the behavior of a linear damper, indicating a the dependency of the component behavior to the amplitude and frequency of the excitation.
The post-processing of the experimental results allows to compute the complex dynamic stiffness as:

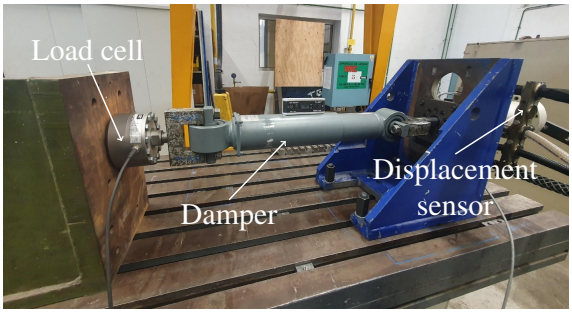

(a)

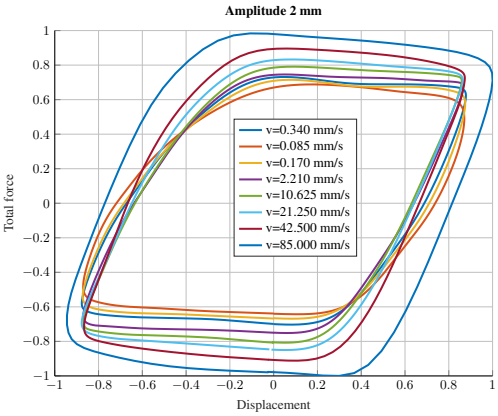

(b)

Figure 1: Experimental study of a yaw damper : (a) Experimental bench for the characterization of the damper (b) Force-displacement hysteresis curves under an applied displacement of $2\,\mathrm{mm}$.

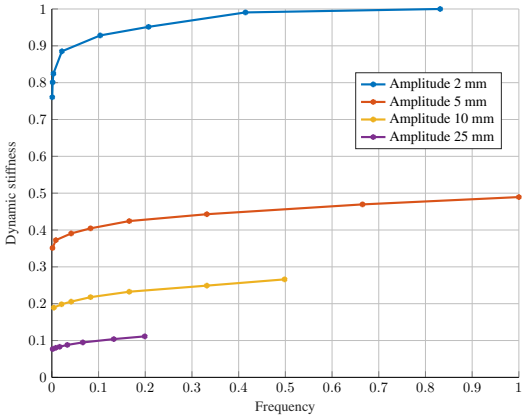

(a)

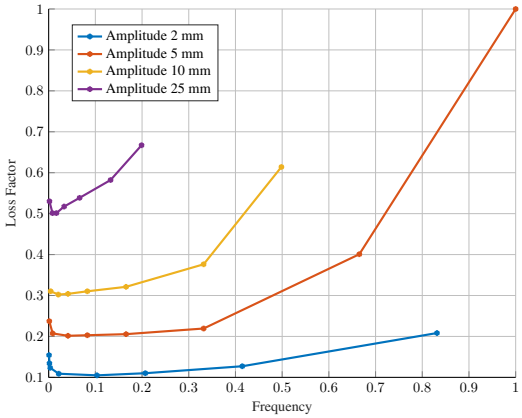

(b)

Figure 2: Evolution of the dynamic stiffness and loss factor as a function of the frequency at various amplitudes. (a) Dynamic stiffness; (b) Loss factor.

$$K_d = |H(\omega)_{|\omega 0}| \tag{1}$$

$$\tan\phi = \frac{\Im[H(\omega)_{|\omega 0}]}{\Re[H(\omega)_{|\omega 0}]} \tag{2}$$

where $H(\omega) = \frac{F(\omega)}{X(\omega)}$ denotes the transfer function in the frequency domain, $\omega 0$ is the frequency of the excitation, and $\Re[*]$ and $\Im[*]$ respectively denote the real and imaginary parts of a complex number. $F(\omega)$ and $X(\omega)$ are the Fast Fourier Transforms of the measured force and displacement at a fixed amplitude and frequency. In the nonlinear domain where the response to a mono-harmonic excitation is multi-harmonic, the values of the dynamic stiffness modulus and of the loss factor are computed at the response's first harmonic. Figure 2 shows the experimental mechanical characteristics as a function of the frequency for various amplitudes.

Two approaches are considered. First, a physics-based model is developed using a rheological model for the yaw damper. Even if some references introduce 3D geometrical models for such components [2, 3, 4], models based on combination of viscous elements, springs, and dashpots are widely used, and well-adapted

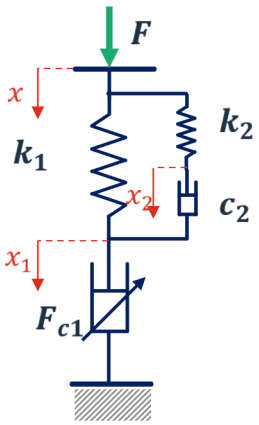

Figure 3: Modeling used for the representation of the yaw damper behavior.

for multibody simulations [5, 6, 7]. An automated procedure is used to determine a set of feasible values for model parameters in order to approximate the measured behavior of the component and a decision-support indicator for the model complexity is introduced. Secondly, a AI-based method is introduced to develop a simplified model, with reduced computational times. Neural networks are an emerging strategy to define input-output relations for complex components presenting nonlinear behaviors [8, 9]. The behavior of the damper is represented by an multi-layer perceptron neural network expressing the complex relationship between force, displacement, velocity and acceleration at the component interfaces and experimental validation is performed in order to evaluate the model's fidelity-to-data.

2 Modeling of the yaw damper using a rheological model

A rheological model inspired by two conventional Maxwell models is used for the yaw damper modeling and is shown on Figure 3. The main element is modified to take into account the nonlinearity of the behavior with the integration of a non linear dashpot characterized by F_{c1} in series with a linear spring of stiffness k_1. A second spring-dashpot element with stiffness k_2 and damping c_2 is connected in a parallel branch to the main stiffness. The system of equations can be written as,

$$F = k_1(x - x_1) + k_2(x - x_2) = F_{c1}(\dot{x}_1) \tag{3}$$

$$k_2(x - x_2) = c_2(\dot{x}_2 - \dot{x}_1) \tag{4}$$

where F is the total force at the extremity of the model. The nonlinear damping F_{c1} of the main Maxwell element is determined using the experimental results measured under the various excitations. For each of the 30 test sets, the minimum and maximum values of the measured force and velocity are retained. This leads to 30 pairs of values $[F_{min}\, v_{min}]$ and 30 pairs of values $[F_{max}\, v_{max}]$ used to defining the force-velocity diagram $[F_{exp}\, v_{exp}]$ shown in Figure 4.

The following expression is used for the definition of a nonlinear force-velocity property curve based on the previous experimental points,

$$F_{c1}(v) = \frac{2}{\pi} \arctan(S\, v)\, F_1 + d\, v + F_2 \tag{5}$$

where the parameters S, F_1, d and F_2 are determined with a fitting method. The final parameter values are given in Table 1 and the approximated curve is shown on Figure 4.

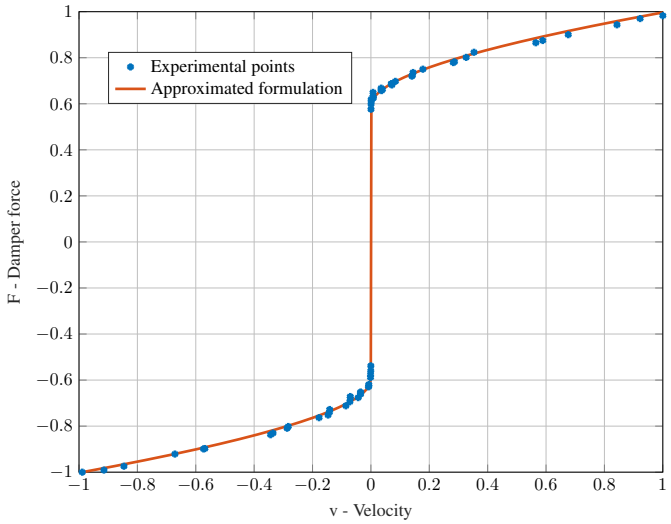

Figure 4: Representation of the nonlinear damping curve expressed by the force as a function of the velocity: the blue points correspond to the experimental values in blue, and the red curve corresponds to the approximation obtained after identification.

Table 1: Identified values for the analytical expression of the force-velocity curve.

S	12 017
F_1	0.65
d	0.38
F_2	-0.0009

3 A complexity level decision support indicator

A complexity level decision support indicator is developed to determine the lowest level of complexity of a model with the highest accuracy required when integrating a component into a larger structure that needs to be validated in accordance with a specified validation plan.

The indicator computation is based on the determination of the sensitivity of an output of interest to the model's characteristics at each step of the validation plan. A high sensitivity value confirms the need to have an accurate model for the component, and further research is required to determine the critical range. It may indicate that further testing is necessary to fine-tune the component's behavior in this range. A low indicator value suggests an opportunity to simplify the model or consider dropping certain characteristic dependencies.

3.1 Determination of feasible values for the linear parameters

The objective of this section is to determine a set of global values for the linear stiffness parameters k_1 and k_2, as well as the linear damping parameter c_2 representative of the behavior of the damper. This research takes the form of an exploratory phase where the three following steps are performed:

1. a sample of k_1 k_2 and c_2 values is generated and integrated in the numerical model,
2. the resulting simulated behavior of the component is computed,
3. the behavior is compared to the measured behavior using quantitative criteria. The sample is retained if the values of the criteria are within predetermined limits.

The dependency towards the amplitude and the frequency of the external solicitation is qualified by the dynamic stiffness modulus and the loss factor. Nevertheless, these two mechanical criteria are not enough to characterize the shape of a force-displacement hysteresis curve in the nonlinear domain and a new criteria involving the force-displacement hysteresis shape is added for the automation of the third step.

3.1.1 The exploratory phase

The set of tested $\{k_1, k_2, c_2\}$ values is created from an initial triplet $\{k_{1_0}, k_{2_0}, c_{2_0}\}$ arbitrarily defined, based on an identification method for one of the experimental configurations, or based on the average of the experimental dynamic stiffness modulus. A Monte Carlo sampling procedure is retained for the definition of the parameter variations around this initial point, ensuring to explore a larger domain than with a random sampling procedure (step 1). The bounds of the parameter relative variations are also chosen in one or several attempts confirming the exploratory nature of this phase.

For a given set of parameters $\{k_1, k_2, c_2\}$, the equations (3) and (4) defining the output force of the enriched Maxwell model are solved using one of the algorithms provided by MATLAB for the resolution of a system of nonlinear differential equations (step 2). This operation is done for each of the 30 test sets and the measured displacements are used as the excitations to get as close as possible to the experimental behavior.

The force is then post-processed and the dynamic stiffness modulus and the loss factor are computed with the formulations given in equations (1) and (2), and compared to the experimental values. The shapes of the force-displacement hysteresis curves are also compared to the experimental ones with the computation of the shape-based criteria. The definition of limits on the elastodynamic characteristics and on the shape-based criteria enables the filtering of the simulated behavior too far from the experimental behavior.

3.1.2 Feasible values for the linear parameters

The previous sequence is applied from the initial set of normalized parameter values $\{k_1 = 1, k_2 = 1, c_2 = 1\}$, a log-variation in the range [0.05 20] and a generation of sample of size 800. The filtering limits of the

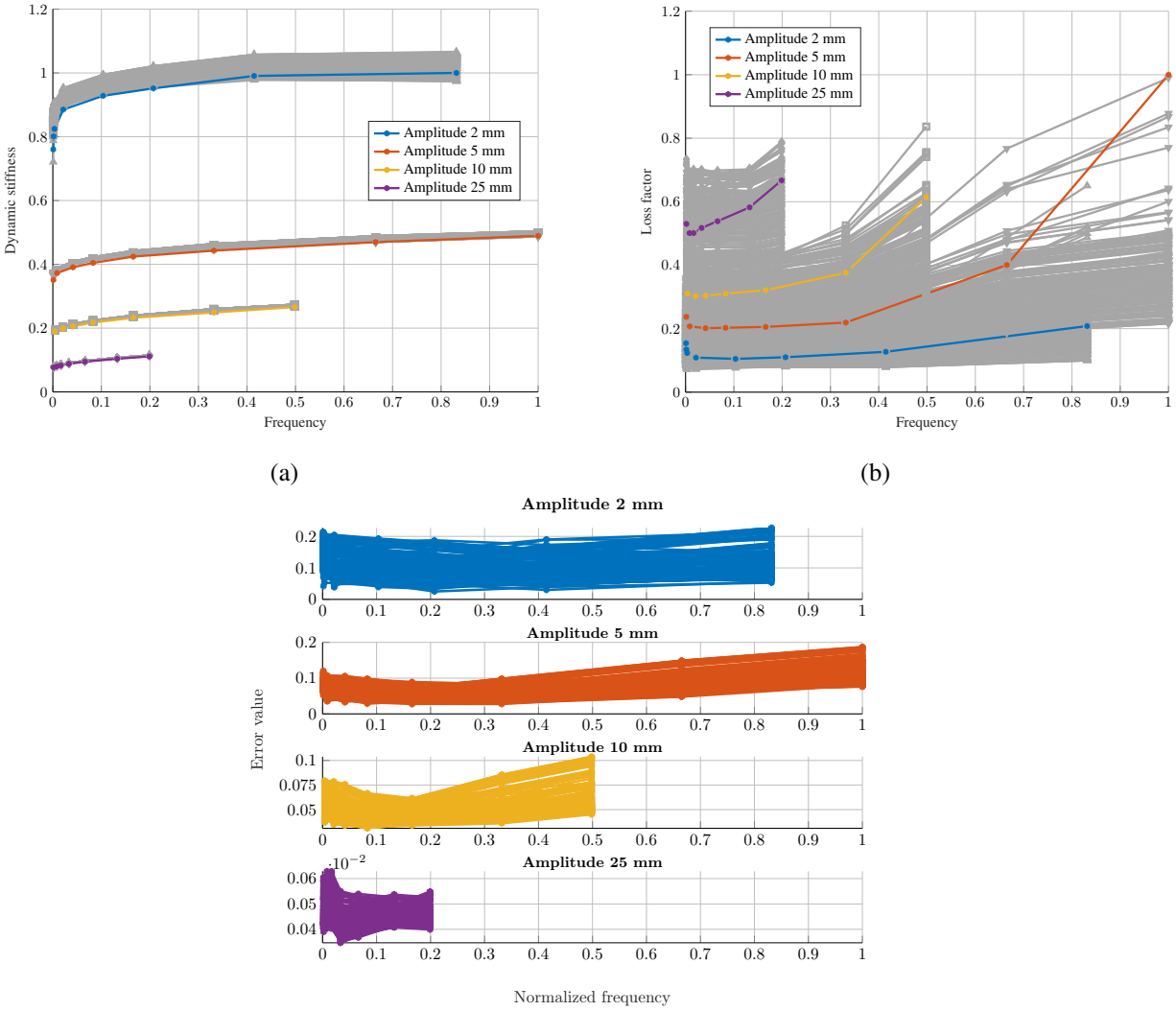

Figure 5: Comparison of the values of the filtering criteria for the feasible parameter values, in grey, and the experimental values, in color. (a) Dynamic stiffness modulus (b) Loss factor (c) Force-displacement shape-based criteria.

elastodynamic characteristics are set to $\pm 50\%$ for the dynamic stiffness modulus, $\pm 30\%$ for the loss angle and $\pm 30\%$ for the force-displacement shape-based criteria.
The application of the selection procedure leads to a final number of 136 sets of feasible values for the linear parameters obtained after the filtering phase, i.e. 17% of the initial sample. Figure 5 shows the stiffness dynamic modulus, the loss factor and the shape-based criteria for the sample. Table 2 gives the maximum variations recorded in comparison to the maximum variations allowed demonstrating that the limit has been reached for the loss factor.

4 Modeling of the yaw damper using a neural network model

Based on the validation plan and the overall model size, the determination of the optimal level of complexity for a structure's components may take some time to achieve. It is then convenient to work on an alternative modeling to avoid this step. Given the overall experimental data resulting from the 30 tests at various amplitudes and frequencies under a mono-harmonic excitation, the aim of this section is to express the instan-

Table 2: Limits defined for the selection of the retained parameters values (step 3 of the procedure).

	Allowed variation	Max variation in the feasible sample
Dynamic stiffness modulus	$\pm 50\%$	14.8 %
Loss angle	$\pm 30\%$	30.0%
Shape-based criteria	$\pm 30\%$	22.7%

Table 3: Options defined for the training of the neural network using the Adam optimizer.

Number of epochs	3 000
Initial learn rate	0.001
Validation frequency	50
Learn rate schedule	piecewise
Lear rate drop factor	0.9
Learn rate drop period	100
L2 regularization	1e-5
Mini batch size	10 000

taneous forces F as a function of the instantaneous displacements x, the velocities v and the accelerations a, dropping the reference to the time step:

$$F = g(x, v, a) \tag{6}$$

where g is a function to determine. The use of artificial neural networks is one way to achieve this goal.

4.1 The multi layer perceptron neural network

The architecture of a multi layer perceptron (MLP) neural network is a succession of hidden layers composed of neurons allowing to transform the data of the input layer to the data of the output layer. The neurons are fully connected, meaning that a neuron of a layer is connected to every neurons of the following layer. The number of layers and the number of neurons per layers are two hyperparameters to determine, defining the number of variables that should be computed during the training phase. This phase corresponds to the solving of the optimization problem where the variables of the neural network are determined. The use of the Deep Learning Toolbox of MATLAB enables to set up the architecture of the neural network and to train it.

4.2 Architecture and training of the neural network

After several tests, the final architecture of the proposed model is composed of 3 inputs in the input layer: the instantaneous displacement x, velocity v and acceleration a, 6 hidden layers, 30 neurons per hidden layer, 1 output in the output layer: the instantaneous force F. The Rectified Linear Unit (ReLU) function is selected as the activation function. Since the 30 data sets have a different number of values, their contents are interpolated to get 6 000 points in each one leading to 180 000 input values for the neural network. The whole set of input values is splitted in the training data and the validation data in the proportion 80-20 and the Adam (adaptative moment estimator) optimizer is chosen with the settings given in Table 3 for the training phase.

4.3 Validation of the neural network model

The neural network model that defines the behavior of the component, i.e. the force as a function of the displacement, velocity and acceleration is finally validated using the original experimental data sets. Using the EEARTH (Enhanced Error Assessment of Response Time Histories) metric introduced in [10], a score

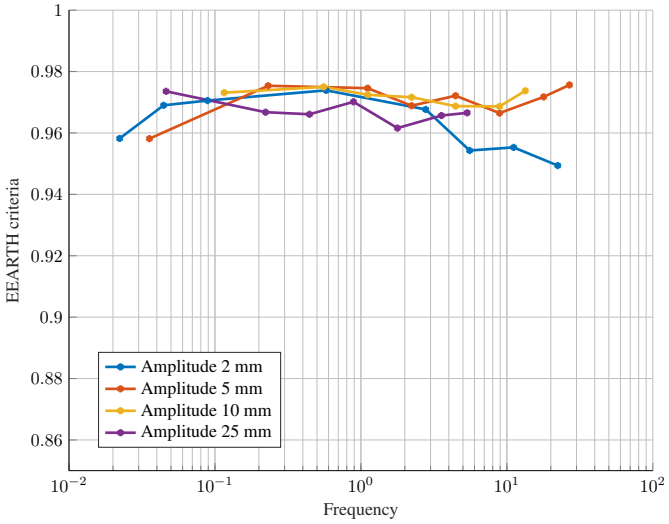

Figure 6: Validation of the neural network with the computation of the EEARTH criteria for the 30 sets as a function of the excitation frequency.

is calculated for each data set to quantify the distance between the experimental and simulated forces. It is expressed as the weighted sum of three scores evaluating the difference in terms of magnitude, phase shift, and slope of two signals,

$$E = w_m E_m + w_p E_p + w_s E_s \tag{7}$$

where E_m, E_p and E_s are respectively the magnitude, phase shift and slope scores and whose the calculation method is explained in [10] and w_a, w_p and w_s are their respective weights with $w_m + w_p + w_s = 1$. A value of 1 indicates a perfect correlation between the signals.

Figure 6 shows the EEARTH criteria computed for the 30 data sets as a function of the excitation frequency and the y-axis minimum limit is set to 0.7. The values are based on the following ratio weights:

$$w_m = 0.2 \quad w_p = 0.4 \quad w_s = 0.4 \tag{8}$$

The scores,which range from 0.949 to 0.976, demonstrate that the neural network model accurately captures the behavior of the component on the measured domain.

5 Conclusion

A method for the search of the level of complexity required to validate a model in railway dynamics has been presented. It relies on the determination of a decision-support indicator based on sensitivity analyses and it is applied to a yaw damper rheological model mounted on a motor bogie. A model developed using a multi-layer perceptron neural network has been introduced that fully represents the component behavior within its training domain. The use of this type of black-box modeling disregarding any physical characteristics and time efficient is a good alternative when it comes to finding an acceptable compromise between the model complexity and the computational load.

References

[1] R. Platz, X. Xu, and S. Atamturktur, “Introducing a round-robin challenge to quantify model form uncertainty in passive and active vibration isolation,” in Model Validation and Uncertainty Quantification,

Volume 3, R. Platz, G. Flynn, K. Neal, and S. Ouellette, Eds. Cham: Springer Nature Switzerland, 2024, pp. 1–4.

[2] C. Huang and J. Zeng, "Dynamic behaviour of a high-speed train hydraulic yaw damper," Vehicle System Dynamics, vol. 56, no. 12, pp. 1922–1944, Dec. 2018. [Online]. Available: https://www.tandfonline.com/doi/full/10.1080/00423114.2018.1439588

[3] A. Alonso, J. G. Giménez, and E. Gomez, "Yaw damper modelling and its influence on railway dynamic stability," Vehicle System Dynamics, vol. 49, no. 9, pp. 1367–1387, Sep. 2011. [Online]. Available: http://www.tandfonline.com/doi/abs/10.1080/00423114.2010.515031

[4] W. L. Wang, Y. Huang, X. J. Yang, and G. X. Xu, "Non-linear parametric modelling of a high-speed rail hydraulic yaw damper with series clearance and stiffness," Nonlinear Dyn, vol. 65, no. 1-2, pp. 13–34, Jul. 2011. [Online]. Available: http://link.springer.com/10.1007/s11071-010-9871-7

[5] Y. Dongxiao, C. Maoru, C. Wubin, and W. Xun, "Study on piecewise linear model of anti-yaw damper and test analysis." Atlantis Press, 2015.

[6] W. Teng, H. Shi, R. Luo, J. Zeng, and C. Huang, "Improved nonlinear model of a yaw damper for simulating the dynamics of a high-speed train," Proceedings of the Institution of Mechanical Engineers, Part F: Journal of Rail and Rapid Transit, vol. 233, no. 7, pp. 651–665, Aug. 2019. [Online]. Available: http://journals.sagepub.com/doi/10.1177/0954409718804414

[7] I. La Paglia, L. Rapino, F. Ripamonti, and R. Corradi, "Modelling and experimental characterization of secondary suspension elements for rail vehicle ride comfort simulation," Proceedings of the Institution of Mechanical Engineers, Part F: Journal of Rail and Rapid Transit, vol. 238, no. 1, pp. 38–47, Jan. 2024. [Online]. Available: http://journals.sagepub.com/doi/10.1177/09544097231178858

[8] M. Burnett, A. Dixon, and J. Webb, "Damper modelling using neural networks," Auto Technology, Apr. 2003.

[9] R. Koganei, K. Sasaki, and N. Watanabe, "Characteristic identification of oil dampers for railway vehicles using Neural Networks," Toledo, Spain, Aug. 2008, pp. 725–733. [Online]. Available: http://library.witpress.com/viewpaper.asp?pcode=CR08-070-1

[10] Z. Zhan, Y. Fu, and R.-J. Yang, "Enhanced Error Assessment of Response Time Histories (EEARTH) Metric and Calibration Process," Apr. 2011, pp. 2011–01–0245. [Online]. Available: https://www.sae.org/content/2011-01-0245/